Int. J. Mech. Sci. Vol. 22, pp. 419–430
Pergamon Press Ltd., 1980. Printed in Great Britain

UPPER-BOUND ANISOTROPIC YIELD LOCUS CALCULATIONS ASSUMING ⟨111⟩-PENCIL GLIDE

ROGER W. LOGAN† and WILLIAM F. HOSFORD
Department of Materials and Metallurgical Engineering, University of Michigan, Ann Arbor, MI 48109, U.S.A.

(*Received* 2 *July* 1979; *in revised form* 26 *January* 1980)

Summary—Deformation by ⟨111⟩-pencil glide has been analyzed by an upper-bound model which combines a least-shear analysis and Piehler's maximum virtual work analysis. The least-shear analysis gives exact solutions if three ⟨111⟩ slip systems are active, while the maximum work analysis provides solutions for the case of four active slip systems. Independent checks are used to determine which solution method is appropriate.

Computer calculations using this model have been made to determine; (1) the orientation dependence of the Taylor factor for axisymmetric deformation; (2) the yield loci for textured materials having [100], [110] and [111] sheet metals and rotational symmetry; (3) the isotropic yield locus for randomly oriented materials; and (4) flow stresses along critical loading paths for various assumed textures with rotational symmetry. The latter calculations indicate that anisotropic yield loci of textured bcc metals with rotational symmetry are much better approximated by

$$\sigma_x^a + \sigma_y^a + R|\sigma_x - \sigma_y|^a = (R+1)Y^a$$

where R is the strain ratio and Y is the tensile yield strength with an exponent $a = 6$ rather than with $a = 2$ as postulated by Hill. It is not known how well upper-bound calculations like these represent actual yielding behavior.

NOTATION

x, y, z	external coordinate axes
$1, 2, 3$	cubic crystal axes, [100], [010] and [001]
$2', 3'$	[110] and [1$\bar{1}$0] axes
θ, ϕ, α	angles describing orientation of x, y, z relative to $1, 2, 3$
M	Taylor factor $= dw/\tau\, d\epsilon_z = \sigma_z/\tau$
W	plastic work per volume
τ	critical shear stress for slip
σ_i	normal stress along i axis
ϵ_i	normal strain along i axis
τ_{ij}	shear stress on ijk coordinate system
τ_i	shear stress on slip system i
γ_{ij}	shear strain on ijk coordinate system
γ_i	shear strain on slip system i
γ_T	sum of absolute magnitudes of γ_i
ψ_i	angle describing rotation of slip plane normal, i, about the slip direction
a, b, c, d	slip plane normals for the ⟨111⟩ slip directions
A, B, C, F, G, H	generalized stress state along cubic axes $1, 2, 3$
A', B', C', D', E'	generalized strain state along $1, 2', 3'$ axes
C_p, D_p, E_p	terms describing strain state
$\chi, \lambda, \psi, \xi, \beta$	ratios of yield strengths along several critical loading paths
F, G, H, A, B, C	constants in generalized yield criteria
Y	yield strength in uniaxial tension along x
ρ	imposed strain ratio $= -\epsilon_y/\epsilon_x$
r	strain ratio, $-\epsilon_y/\epsilon_x$ in uniaxial tension
R	strain ratio, $\epsilon_y/\epsilon_z = r/(1-r)$ in uniaxial tension
a, m, n	exponents in generalized yield criteria

INTRODUCTION

Recently there has been a considerable interest in mathematical modeling and computer simulation of sheet metal forming, especially with low-carbon steel. Such modeling requires satisfactory constitutive relations. Hill's anisotropic yield

†This paper is based on a senior project of Mr. Logan who is now a graduate student at the University of California (Davis).

criterion[1] has been widely used, but there are reasons to doubt how accurately it describes the anisotropic behavior. An alternative approach is to calculate yield loci from considerations of crystallographic texture and the crystallographic nature of slip. For low carbon steel and other bcc metals ⟨111⟩-pencil glide is a good description of the slip behavior. While it can be shown that for a given crystal orientation the plastic anisotropy with ⟨111⟩-pencil cannot differ more than 15% from that with ⟨111⟩{110} slip, this is not a good enough apiroximation for mathematical modeling of sheet forming of low carbon steel.

Upper-bound calculations of anisotropy are based on assuming the same shape change in each grain. For fcc metals two methods of calculation have been used. One has been an extension of Bishop and Hill's analysis[2] which is focused on the limited number of stress states capable of producing the multiple slip required for an arbitrary shape change of a grain. The principle of maximum virtual work is used to identify the correct stress state for producing the required shape change in each grain. The other approach is based on Taylor's analysis. All combinations of five independent slip systems are considered and that combination which can produce the shape change with the least shear (and hence actual work) is identified. Although the computational strategies of the two methods are very different, the results are identical.

Much less work has been done in analyzing the pencil-glide model. Using a Taylor least-work analysis, Chin *et al.*[4, 5] and Hutchinson[6] approximated pencil glide by assuming slip on any of a large but finite number of slip planes containing the ⟨111⟩ directions. These planes differ in orientation by small rotations about the ⟨111⟩ slip directions. Examining all independent combinations of five such slip systems, they selected the one for which the work is the least. Chin has calculated the orientation dependence of strength under axisymmetric flow and Hutchinson reported the yield locus shape for a randomly oriented polycrystal.

A minimum of five independent slip variables are required to produce an arbitrary shape change in a crystal. If slip is restricted to specific crystallographic planes and directions, these variables must be the amount of shear strain on each of five active slip systems, so a minimum of five active slip systems are required. With pencil glide, however, there are two variables associated with each slip system; the orientation or angular rotation of the slip plane about the ⟨111⟩ direction as well as the shear strain. Therefore, a minimum of three active slip systems are required.

Penning[7] described an exact solution for pencil glide based on a least work (Taylor-type) analysis. He treated both the case of three and four active slip directions. Parniere and Sauzay[8] also described pencil glide calculations based on a least work analysis. Their upper-bound locus for randomly oriented material shows less strengthening under plane-strain than predicted by von Mises and their locus for a sharp {111}⟨110⟩ texture indicates much less strengthening under biaxial tension than would be predicted by the Hill theory for the same R-value. The Penning analysis has been applied to calculation of upper-bound yield loci from orientation distribution functions[9].

Piehler *et al.*[10–12] approached the problem in a way analogous to Bishop and Hill by considering the stress states capable of activating enough slip systems to satisfy an arbitrarily imposed strain state and showed that there are eight independent variables, namely the orientations of the four active slip planes and the magnitudes of the four shear strains, while if three ⟨111⟩ directions are active there are six independent variables. He derived expressions for the stress states for the four slip system case. However, he was unable to derive general expressions for the three slip system case, so instead of a general solution, he used a limited number of specific solutions. For each assumed shape change, the stress state corresponding to the largest virtual work was selected as appropriate. The method was applied to calculating the orientation dependence of the M-factor ($M = \mathrm{d}w/\tau\,\mathrm{d}\epsilon_x = \sigma_x/\tau$) for axisymmetric deformation about x, and to calculating yield loci for sheet textures with rotational symmetry about common sheet normals of ⟨111⟩, ⟨011⟩ and ⟨001⟩. However, these results must be regarded as approximate in view of the way the three slip system case was treated.

Recently Morris *et al.*[13, 14] have derived exact solutions for a maximum virtual work analysis of pencil glide and applied their analysis to calculation of yield loci from orientation distribution functions.

CALCULATION METHOD

The present calculation employs both the maximum virtual work and the least-shear upper-bound solution methods. For the four slip system case Piehler's stress states and the principle of maximum virtual work are used to identify the appropriate stress state. This solution is valid, however, only if the implied shear strains on the four slip systems may be achieved with an internal energy dissipation equal to the external work.

Taylor's least-shear principle is used for the three slip system solution. Five independent equations relate the external strain to the four shear strains, γ_i, and four angular rotations of the slip plane normals, ψ_i. By setting one of the shear strains equal to zero, six variables remain (three angular orientations of the slip planes and three shear strain). One of the remaining angular orientations is fixed and the shear strains required to satisfy the imposed strain are determined and $\gamma_T = \Sigma|\gamma_i|$ is found. The angular orientation, ψ_i, is then given a new value and the process repeated until the minimum value of γ_T possible with these tress slip directions is found. This procedure is then repeated with each of the slip directions in turn being inactive to identify the three slip direction solution requiring the least shear. However, this solution is appropriate only if the stress state necessary to activate the three slip systems does not cause a shear stress on the fourth system exceeding the critical value for slip.

Since one and only one of the two possibilities (four slip systems or three slip systems) is correct, we first assume the three slip system solution, and determine whether this solution is appropriate. If it is not appropriate the four slip system solution is used. Alternately, the four slip system solution could be checked, but it was found in preliminary calculations that it always checked when the three slip system solution was inappropriate.

The soundness in the combination of these two principles lies in the fact that checks are available for both solutions. The least-work analysis eliminates the problem of identifying all necessary stress state groups for simultaneous slip in three directions, while the maximum virtual work principle avoids the very complicated least work analysis for the four active system case.

Shear strains on slip systems

A set of imposed external strains, ϵ_x, ϵ_y and ϵ_z (with $\gamma_{yz} = \gamma_{zx} = \gamma_{xy} = 0$) are assumed. The crystal orientation is described by the latitude, ϕ, and the longitude, θ, of z axis relative to the 1 = [100], 2 = [010] and 3 = [001] crystal axes and by an angular rotation, α, of the x and y axes about z (see Fig. 1). The strains on the x, y, z axis system are transformed to strains on the 1, 2, 3 axis system and these in turn transformed to the strain on the 1, 2′, 3′ system where 2′ = [011] and 3′ = [0$\bar{1}$1]. Finally, the strains on the 1, 2′, 3′ axes may be expressed in terms of the shear strains on the four slip systems by five independent equations with eight unknowns.

$$A' = -(3/\sqrt{2})\epsilon_{2'} = \gamma_b \cos\psi_b + \gamma_d \cos\psi_d \quad (1)$$

$$B' = -(3/\sqrt{2})\epsilon_{3'} = \gamma_a \cos\psi_a + \gamma_c \cos\psi_c \quad (2)$$

$$C' = (\sqrt{6}/2)\gamma_{2'3'} = -\gamma_a \sin\psi_a + \gamma_b \sin\psi_b - \gamma_c \sin\psi_c + \gamma_d \sin\psi_d \quad (3)$$

$$D' = 3\gamma_{3'1} = \gamma_a \cos\psi_a + \sqrt{3}\gamma_b \sin\psi_b - \gamma_c \cos\psi_c - \sqrt{3}\gamma_d \cos\psi_d \quad (4)$$

$$E' = 3\gamma_{1'2'} = \sqrt{3}\gamma_a \sin\psi_a + \gamma_b \cos\psi_b + \sqrt{3}\gamma_c \sin\psi_c - \gamma_d \cos\psi_d \quad (5)$$

where γ_a, γ_b, γ_c and γ_d are the shear strains on the four slip systems and ψ_a, ψ_b, ψ_c and ψ_d describe the orientations of the four slip planes (see Fig. 2).

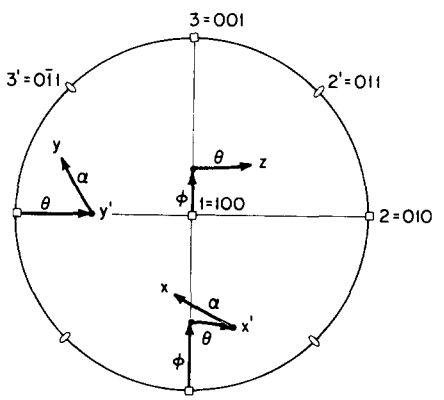

FIG. 1. Stereographic representation of the axis system.

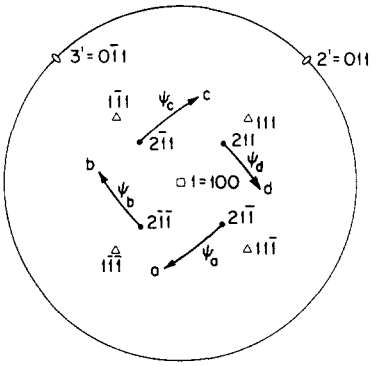

FIG. 2. Stereographic representation of the pencil glide systems. a, b, c and d are the slip plane normals for slip directions [1$\bar{1}$1], [111], [11$\bar{1}$] and [1$\bar{1}$1] respectively.

Least shear (three slip systems)

If only three slip systems are active there are only six unknowns on the right hand side of equations (1)–(5). For example, if we assume $\gamma_a = 0$, these equations simplify to

$$\gamma_c = B'/\cos\psi_c \tag{6}$$

$$\gamma_b = \sqrt{[(D_p + C_p)^2 + (E_p + A')^2]}/2 \tag{7}$$

$$\gamma_d = \sqrt{[(D_p - C_p)^2 + (E_p - A')^2]}/2 \tag{8}$$

where $C_p = C' + \gamma_c \sin\psi_c$, $D_p = (D' + B')/\sqrt{3}$ and $E_p = E' - \sqrt{3}\gamma_c \sin\psi_c$.

A value of ψ_c is assumed and equations (6)–(8) solved for the shear strains γ_b, γ_c and γ_d and the total shear strain $\gamma_T = |\gamma_b| + |\gamma_c| + |\gamma_d|$. The angle ψ_c is varied using a "golden-section search"[15] to minimize γ_T and values of ψ_b, ψ_c and ψ_d at the minimum are noted.

The next step is to find the corresponding stress state, $A = \sigma_2 - \sigma_3$, $B = \sigma_3 - \sigma_1$, $C = \sigma_1 - \sigma_2$, $F = \tau_{23}$, $G = \tau_{31}$ and $H = \tau_{12}$. Equations (9)–(16) were developed by writing expressions for the four values of τ_i in terms of the stress state and ψ_i and setting $d\tau_i/d\psi_i = 0$ to find the orientation ψ_i corresponding to the largest value of τ_i.

$$\tau_a \sin\psi_a = (A - G - H)/\sqrt{6} \tag{9}$$

$$\tau_a \cos\psi_a = (C - B - H + G + 2F)/(3\sqrt{2}) \tag{10}$$

$$\tau_b \sin\psi_b = (-A + G - H)/\sqrt{6} \tag{11}$$

$$\tau_b \cos\psi_b = (C - B + H + G - 2F)/(3\sqrt{2}) \tag{12}$$

$$\tau_c \sin\psi_c = (A + G + H)/\sqrt{6} \tag{13}$$

$$\tau_c \cos\psi_c = (C - B + H - G + 2F)/(3\sqrt{2}) \tag{14}$$

$$\tau_d \sin\psi_d = (-A - G + H)/\sqrt{6} \tag{15}$$

$$\tau_d \cos\psi_d = (C - B - H - G - 2F)/(3\sqrt{2}). \tag{16}$$

Now letting the critical shear stress for slip be unity, so $\tau_b = \tau_c = \tau_d = 1$, equations (11)–(16) are solved for the values of A, B, C, F, G and H. With these values the level of τ_a is determined using equations (9) and (10). If $|\tau_A| \leq 1$, the solution is appropriate. Otherwise, the remaining cases of simultaneous slip on three systems are examined in a similar manner. If none are found appropriate this implies that four slip systems are active.

Maximum virtual work (four slip systems)

Piehler[11] showed that the stress state must satisfy the equation

$$F^2(B - C) = G^2(C - A) = H^2(A - B) = 0 \tag{17}$$

for four systems to operate simultaneously, and found four general solutions (equations (1), (3a), (3b) and (3c) in Ref. [11]) which are expressed in terms of the strain on the 1, 2, 3 axis system. The appropriate stress state is that one which gives the largest value of dw, where

$$dw = -B\,d\epsilon_1 + A\,d\epsilon_2 + F\,d\gamma_{23} + G\,d\gamma_{31} + H\,d\gamma_{12}. \tag{18}$$

The maximum virtual work solution can also be checked for consistency. Since the shear stresses on all four systems must be equal, equations (6)–(13) yield the slip plane angles. Equations (1)–(5) may then be solved for the shear strains on the individual system. If the solution is correct, the sum of the magnitude of the shear strains will equal the external work from equation (18). Otherwise, the calculated stress state will not produce the imposed strains.

The value of virtual work calculated for the four slip system case always lies below the least shear solution for the three slip system solution, except at points of tangency where the transition from one solution to the other occurs, as shown in Fig. 3.

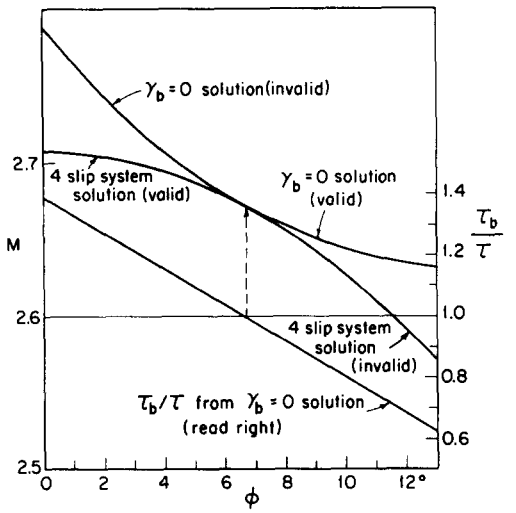

FIG. 3. Calculated Taylor Factor for the three slip system ($\gamma_b = 0$) and four slip system solutions as a function of ϕ for $\theta = 25°$. The ratio of τ_b/τ is also shown. The $\gamma_b = 0$ solution is valid for $\tau_b/\tau \leq 1$ (i.e. $\phi \geq 6{\cdot}75$) while the four-slip solution is appropriate for $\tau_b \geq 1$.

APPLICATIONS

The computer program based on these analyses was applied to four problems; the orientation dependence of the Taylor factor for axisymmetric deformation; the yield loci for sheets having rotationally symmetric texture about sheet normals of [001], [011] and [111]; the isotropic yield locus for randomly oriented grains; and finally a few critical parameters describing the yield loci shapes of a large number of randomly chosen textures with rotational symmetry.

Taylor factor for axisymmetric deformation

Values of the Taylor factor, $M = \mathrm{d}w/\tau\,\mathrm{d}\epsilon_z$, for the axisymmetric deformation ($\epsilon_x = \epsilon_y = -1/2\epsilon_z$, $\gamma_{yz} = \gamma_{zx} = \gamma_{xy} = 0$) were calculated for orientations of z varying at one degree increments of θ and ϕ over the basic stereographic triangle. The results, shown in Fig. 4, differ in several places from those of Piehler[12]. The most significant difference is the extension of the region for which [111] is inactive down to $\phi = 0°$ at $\theta = 9{\cdot}75°$.

To calculate the average Taylor factor, randomly oriented material was approximated by 750 orientations. The values of θ and ϕ were chosen randomly within regions described by 25 increments of $\Delta \sin\phi = 0{\cdot}04$ and 30 increments of $\Delta\theta = 1{\cdot}5°$, covering spherical triangle of $0 \leq \theta \leq 45$ and $0 \leq \phi \leq 90$. The

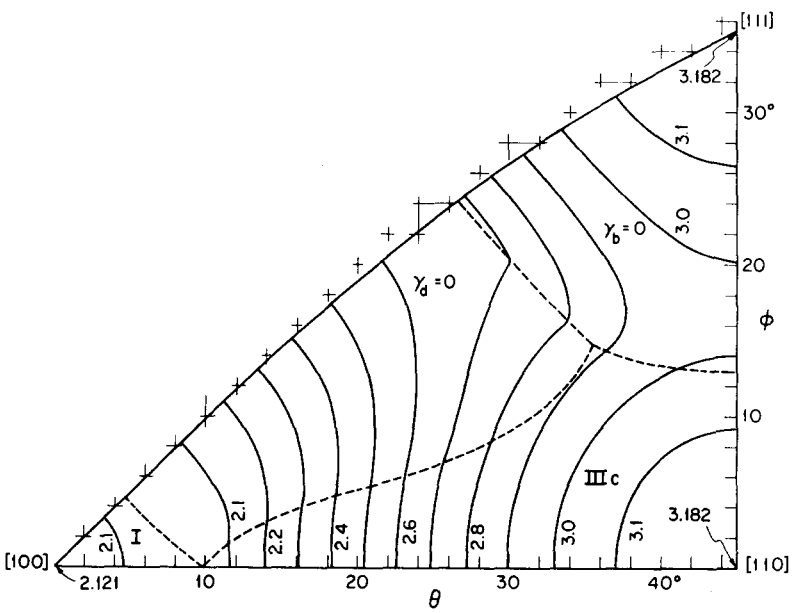

FIG. 4. Orientation dependence of the Taylor Factor, M, over the basic orientation triangle. In regions 1 and 3c, four slip systems are active, while in regions $\gamma_d = 0$ and $\gamma_b = 0$ only three slip systems are active. The average value is $M = 2{\cdot}7398 \pm 0{\cdot}0016$.

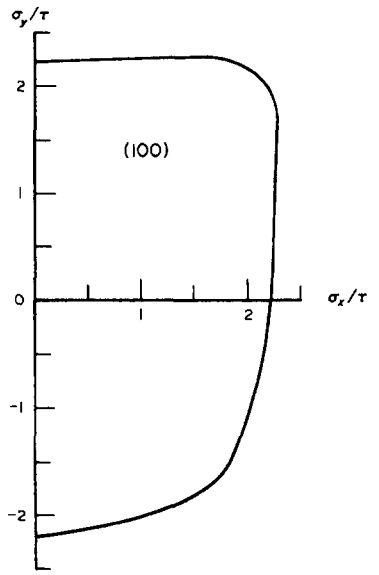

FIG. 5. Yield locus for rotationally symmetric sheets with $z = [100]$. The present calculations coincide with those of Piehler.

calculation was reported five times to allow a t-test of the confidence limit. The average M-value was found to be $2{\cdot}7398 \pm 0{\cdot}0016$ within the 90% confidence limits compared with previously reported values of 2·733 for pencil glide[12], and 2·748 for approximate pencil glide[6], and 2·754 for mixed $\langle 111\rangle$-$\{110\}$, $\{112\}$, $\{123\}$ slip[4, 5].

Yield loci for rotational symmetry about [100], [110] *and* [111]

Yield loci were calculated for orientations of the sheet normal, z, fixed at [100], [110] and [111].

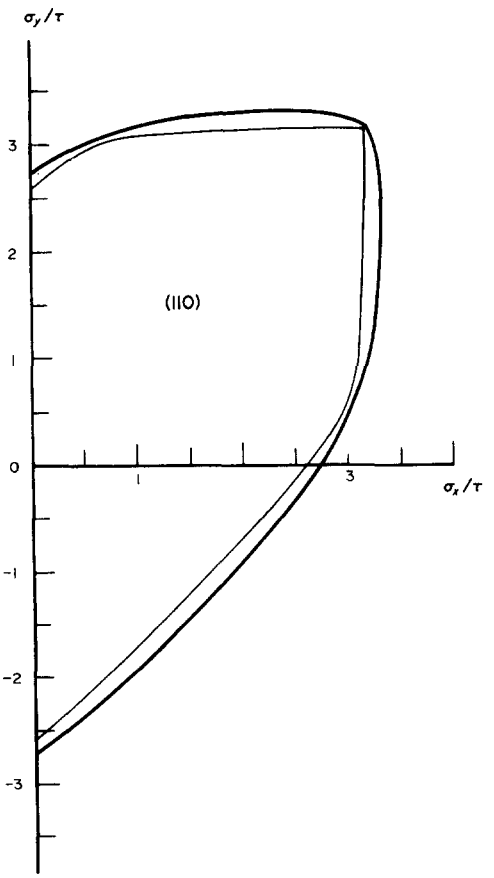

FIG. 6. Yield locus for rotationally symmetric sheets with $z = [110]$. The present calculations are shown by the outer curve while the inner curve is from Piehler.

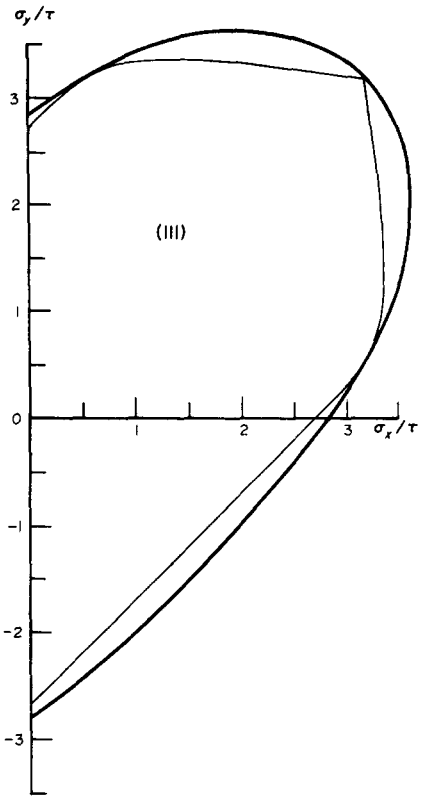

FIG. 7. Yield locus for rotationally symmetric sheets with z = [111]. The present calculations are shown by the outer curve while the inner curve is from Piehler.

Rotational symmetry was approximated by considering orientations differing from one another by rotations of $\Delta\alpha = 3°$ about the sheet normal. The imposed strain ratio $\rho = -\epsilon_y/\epsilon_x$ was varied from -1 to $+1$ in increments of 0·1. For each strain ratio the calculated stress state was converted to the x, y, z system, with $\sigma_z = 0$ and averaged over all the α-values. The strain ratios, R, for uniaxial tension were found by a search for the condition $\sigma_y = 0$. Figs. 5–7 show the yield loci for [100], [110] and [111] sheet normals. For comparison, the yield loci previously calculated by Piehler[12] are also indicated. The values of σ_x/τ for critical loading paths are given in Table 1. For the [100] sheet normal the present results coincide with Piehler's. It is interesting to note that for the [100] calculations less than 1% of the solutions correspond to the three slip system case for which Piehler's analysis is only approximate. In contrast, our [110] and [111] loci differ considerably from Piehler's especially in the first quadrant where our loci lie outside of Piehler's. The three slip system solution was found appropriate for [110] and [111] about 54 and 92% of the times respectively. We found no corner at biaxial tension for [111] and a very much blunter corner for [110].

Isotropic yield locus

A yield locus for isotropic pencil-glide material was calculated by assuming that the material was made up of 900 texture components, with the orientations of these components being chosen randomly from each of 300 regions given by 15 increments of $\Delta\theta = 1·5°$, and 20 increments of $\Delta \sin\phi = 0·05$, covering the spherical triangle $0 \le \theta \le 45°$, $0 \le \phi \le 90°$. For each ϕ and θ, three values of α were also randomly selected within 60° intervals. The calculations were repeated six times with different random numbers so that the 90% confidence limits could be established. The results are shown in Fig. 8, where the boxes indicate the confidence limits and in Table 1. Hutchinson's calculations[6] are shown as solid points. It can be seen that

TABLE 1. VALUES OF σ_x/τ FOR CRITICAL LOADING PATHS

Texture	σ_x/τ Biaxial tension ($\epsilon_y = \epsilon_x$)	σ_x/τ Plane strain ($\epsilon_y = 0$)	$2\sigma_x/\tau$ Plane strain ($\epsilon_y = 0$)	σ_x/τ Uniaxial tension ($\sigma_y = 0$)	Strain ratio $T = \epsilon_y/\epsilon_z$
[100]	2·121	2·288	3·409	2·236	0·105
[110]	3·182	3·317	2·910	2·748	1·714
[111]	3·182	3·626	3·038	2·844	2·632
Random	2·7398 ± 0·0016	3·0647 ± 0·0087	3·065	2·739	1·000

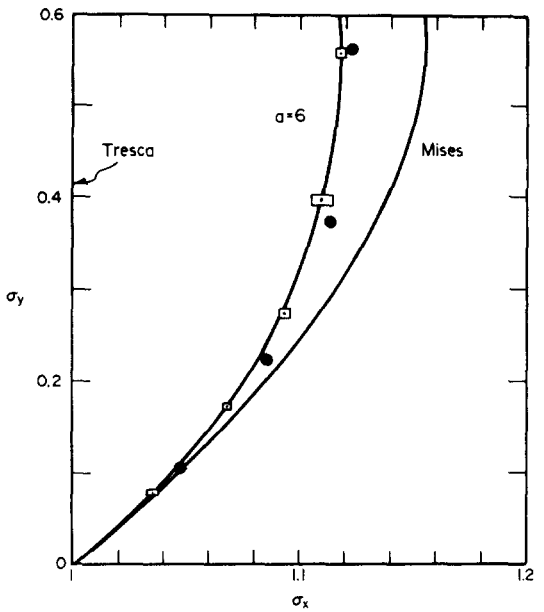

FIG. 8. Isotropic yield locus for randomly oriented material. Note the σ_x scale is expanded. Calculated points are shown by boxes indicating the 90% confidence limits. For comparison, Hutchinson's approximate pencil glide calculations are shown as solid points. The von Mises and Tresca criteria are indicated as well as generalized isotropic criterion with $a = 6$.

the calculated results are very closely fit by an exponent $a = 6$ in a generalized isotropic yield criterion of the form[16, 17]

$$|\sigma_2 - \sigma_3|^a + |\sigma_3 - \sigma_1|^a + |\sigma_1 - \sigma_2|^a = 2Y^a, \tag{19}$$

which reduces to

$$|\sigma_x|^a + |\sigma_y|^a + |\sigma_x - \sigma_y|^a = 2Y^a \tag{20}$$

for plane-stress ($\sigma_z = 0$) loading. The von Mises criterion ($a = 2$) overestimates the strengthening due to biaxiality.

Yield loci for mixed textures with rotational symmetry

To more fully explore the anisotropic characteristics predicted by the upper-bound pencil-glide model, 101 rotationally symmetric textures were considered. In these calculations, real sheet textures were approximated by mixed textures consisting of three texture components, each with a single sheet normal. Rotational symmetry was generated by rotational increments of $\Delta\alpha = 18°$ about each sheet normal, the starting α being randomly chosen to lie between 0 and 18°. The volume fraction of each component and the orientation of its sheet normal, θ and $\sin\phi$, were also randomly chosen.

Instead of exploring the entire yield locus, calculations were made of yield strengths along several critical loading paths: biaxial tension ($\epsilon_y = \epsilon_x$), plane strain ($\epsilon_y = 0$), plane strain ($\epsilon_z = 0$) and uniaxial tension ($\sigma_y = 0$). In the latter case, a search for the $\sigma_y = 0$ conditions produced both the R-value and the yield strength. The ratios of yield strengths along these loading paths,

$$\chi = \sigma_{x(\text{biaxial tension})}/\sigma_{x(\text{uniaxial tension})}$$

$$\lambda = \sigma_{x(\text{plane-strain},\ \epsilon_y=0)}/\sigma_{x(\text{uniaxial tension})}$$

$$\psi = 2\sigma_{x(\text{plane-strain},\ \epsilon_z=0)}/\sigma_{x(\text{uniaxial tension})}$$

$$\xi = \sigma_{x(\text{plane-strain},\ \epsilon_y=0)}/\sigma_{x(\text{biaxial tension})} = \lambda/\chi$$

$$\beta = \sigma_{x(\text{plane-strain},\ \epsilon_y=0)}/2\sigma_{x(\text{plane-strain},\ \epsilon_z=0)} = \lambda/\psi$$

were calculated and plotted against the strain ratio in Figs. 9–13, each solid point represents one texture. The open circles at $R = 1$ are from the calculations of the isotropic yield locus ($\chi = \beta = 1$) and ($\lambda = \psi = \xi = 1{\cdot}1186$). The abscissae are linear in $r = -\epsilon_y/\epsilon_x$ and the corresponding strain ratios $R = \epsilon_y/\epsilon_z$ are shown at the top of each plot.

DISCUSSION

The scatter in these calculations shows that the shapes of the yield loci are not uniquely related to the R-values. The greatest scatter occurs for the parameters χ and ξ which involve biaxial tension. This loading path is furthest removed from uniaxial tension, along which the R-value is defined. Despite the scatter, it is

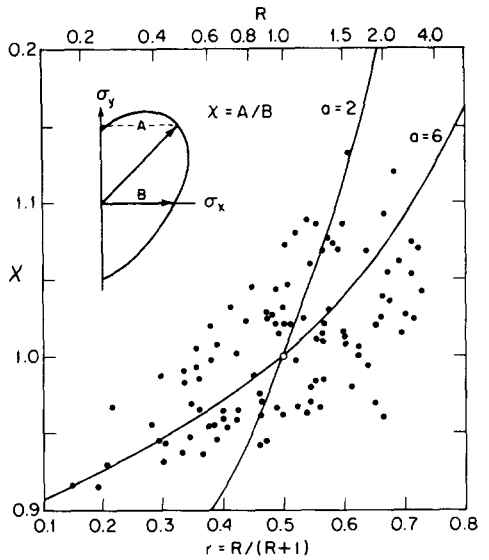

FIG. 9. Dependence of biaxial/uniaxial strength ratio, χ, on the strain ratio, R. Each point is for a randomly chosen rotationally symmetric mixed texture. The Hill theory is shown by the line $a = 2$ and equation (22) by the line $a = 6$.

apparent that the general trends are not well described by Hill's anisotropic yield criterion, which is indicated by the solid lines labelled ($a = 2$) in Figs. 9–13.

Recently an anisotropic yield criterion of the form

$$F|\sigma_y - \sigma_z|^a + G|\sigma_z - \sigma_x|^a + H|\sigma_x - \sigma_y|^a = 1 \tag{21}$$

was suggested[18]. This reduces to Hill's criterion for $a = 2$ and to equation (19) for isotropy. For plane-stress loading and rotational symmetry about z, equation (21) becomes

$$|\sigma_x|^a + |\sigma_y|^a + R|\sigma_x - \sigma_y|^a = (1 + R)Y^a. \tag{22}$$

The general trends in Figs. 9–12 are well described by this criterion with $a = 6$. In similar upper-bound calculations for fcc metals the best fits were obtained with $a = 8$–10. Fig. 14 shows the yield loci shapes for $a = 2$ and $a = 6$ with $R = 0{\cdot}5$ and 2. As a is increased from 2 to 6, the yield loci approach the Tresca criterion.

The scatter of the points in Figs. 9–12 strongly suggests that no yield criterion, without many adjustable parameters could completely describe the calculated results. Our intent is to offer instead a simple yield

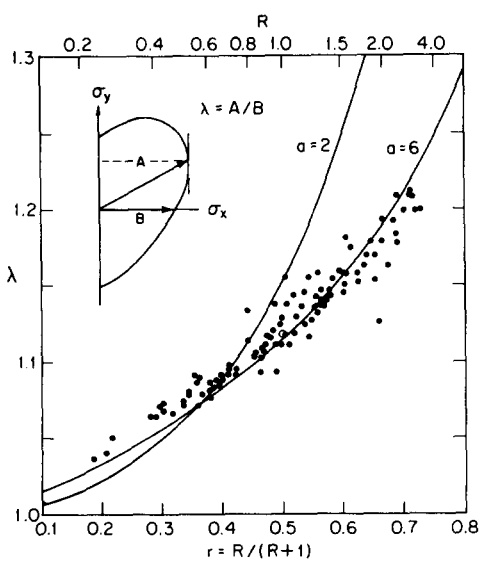

FIG. 10. The dependence of the plane-strain ($\epsilon_y = 0$)/uniaxial strength ratio, λ, on the strain ratio, R. Each point is for a randomly chosen rotationally symmetric mixed texture. The Hill theory is shown by the line $a = 2$ and equation (22) by the line $a = 6$.

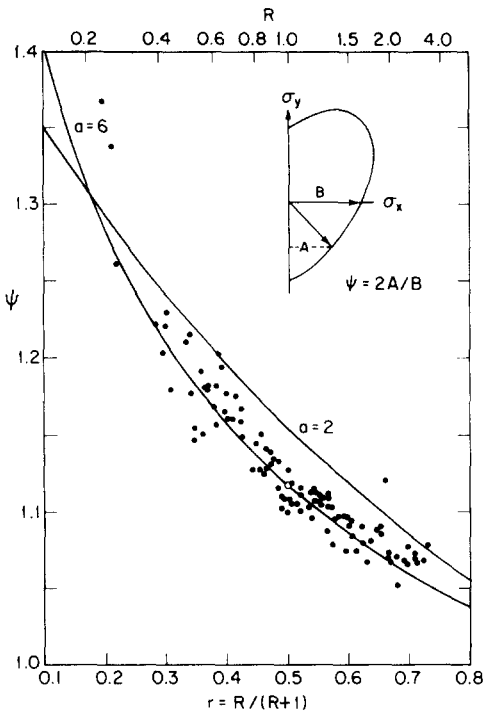

FIG. 11. The dependence of the plane-strain ($\epsilon_z = 0$)/uniaxial strength ratio, ψ, on the strain ratio, R. (Note the plane-strain strength ($\epsilon_y = 0$) equals twice the value of σ_x along that loading path.) Each point is for a randomly chosen rotationally symmetric mixed texture. The Hill theory is shown by the line $a = 2$ and equation (22) by the line $a = 6$.

criterion with a single exponent, a, to approximate the general trends. This criterion requires only experimental values of R and Y, both measurable in a single tension test, to allow prediction of yielding behavior under other loading conditions.

However, it should be recognized that the calculations presented here, and represented by equation (22) are based on an upper-bound model of deformation in which it is assumed that every grain undergoes the same strains. It is not known how well this model describes the yielding behavior of real metals. Other models or experimental data may be better described by other yield criteria or by equation (22) with exponents other than six.

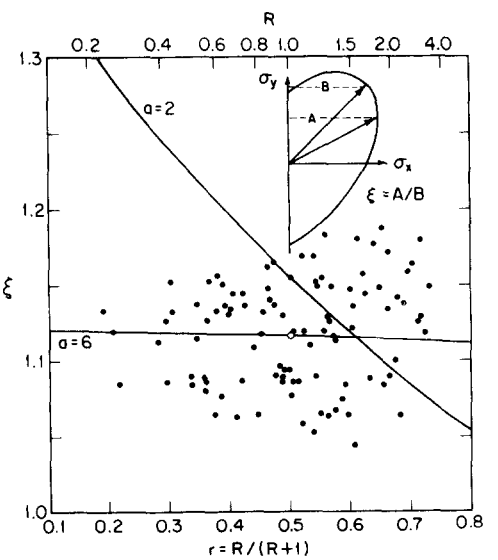

FIG. 12. The dependence of the plane-strain ($\epsilon_y = 0$)/biaxial strength ratio, ξ, on strain ratio, R. Each point is for a randomly chosen rotationally symmetric texture. The Hill theory is shown by the line $a = 2$ and equation (22) by the line $a = 6$.

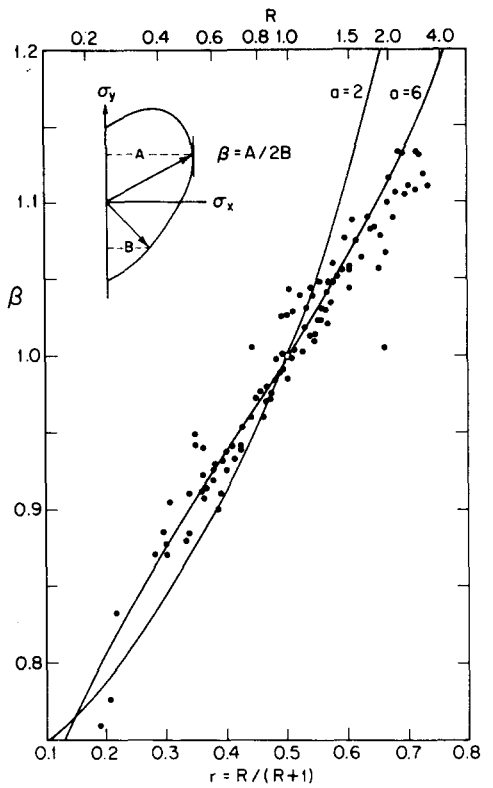

FIG. 13. The dependence of the plane-strain ($\epsilon_y = 0$)/plane-strain ($\epsilon_y = 0$) strength ratio, β, on the strain ratio, R. Each point is for a randomly chosen rotationally symmetric texture. The Hill theory is shown by the line $a = 2$ and equation (22) by the line $a = 6$.

Hill[19] has recently suggested an even more general anisotropic yield criterion

$$F|\sigma_2 - \sigma_3|^m + G|\sigma_3 - \sigma_1|^m + H|\sigma_1 - \sigma_2|^m + A|2\sigma_1 - \sigma_2 - \sigma_3|^m + B|2\sigma_2 - \sigma_1 - \sigma_3|^m + C|2\sigma_3 - \sigma_1 - \sigma_2|^m = Y^m \tag{23}$$

which reduces to equation (21) if $A = B = C = 0$. Several investigators[20–23], working with sheet metals having $\bar{R} < 1$, have derived biaxial stress–strain curves from bulge test data that lie above the uniaxial stress–strain curves for the same materials. These findings of $\chi > 1$ for $\bar{R} < 1$ are surprising and not possible according to either the original criterion or equation (22). Although the upper bound calculations do indicate that $\chi > 1$ for $R < 1$ for some textures (see Fig. 9), this is not the general trend. Some forms of Hill's new

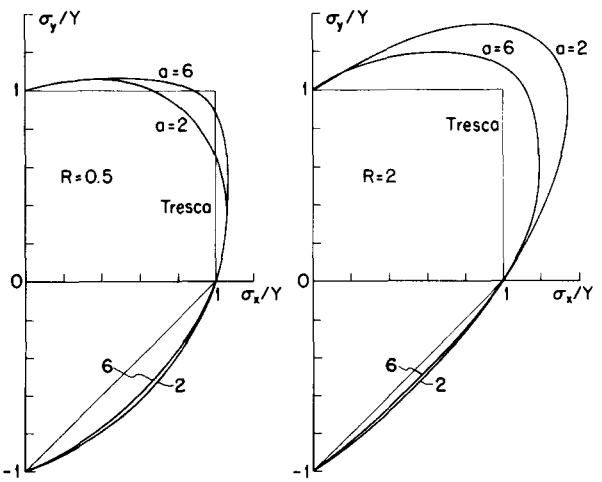

FIG. 14. Comparison of anisotropic yield loci predicted by equation (22) (with $a = 6$) and Hill ($a = 2$) for $R = 0{\cdot}5$ and $R = 2{\cdot}0$.

criterion will permit $\chi > 1$ with $R < 1$ for rotationaly symmetric textures. Parmar and Mellor[22, 23] used one special form with $A = B = F = G = 0$,

$$|\sigma_1 + \sigma_2|^m + (1 + 2R)|\sigma_1 - \sigma_2|^m = 2(1 + R)Y^m \tag{24}$$

to explain the anomalous bulge test data. They found that the ratios of biaxial to uniaxial yield strengths, χ, implied exponents of m from 1·38 to 2·0. It should be noted, however, that a different exponent was needed for each R-value and that no attempt was made to determine whether that exponent described the yielding behavior under other loading paths.

Bassani has made Bishop–Hill type calculations of yield loci for fcc metals with rotationally symmetric textures, and has attempted to fit these with a criterion of the form

$$\left|\frac{\sigma_1 + \sigma_2}{2\sigma_b}\right|^n + \left|\frac{\sigma_1 - \sigma_2}{2\tau}\right|^m = 1 \tag{25}$$

where σ_b and τ are the yield strengths in biaxial tension and in pure shear respectively, where m and n are two adjustable exponents. Both equations (24) and (25) require more than a simple tension test to evaluate the constants.

CONCLUSIONS

1. An upper-bound ⟨111⟩ pencil-glide model has been developed which combines a least-shear analysis for the case of three active slip systems with a maximum virtual work analysis for the case of four active slip systems.

2. Calculated yield loci for both isotropic (random) and randomly chosen mixed textures with rotational symmetry are closely approximated by

$$|\sigma_x|^a + |\sigma_y|^a + R|\sigma_x - \sigma_y|^a = (R + 1)Y^a$$

with $a = 6$. It is not known, however, how accurately the upper-bound model describes actual yielding behavior of bcc metals.

Acknowledgements—The authors wish to acknowledge the financial support of the National Science Foundation and the American Iron and Steel Institute. Mr. C. Vial and Professor W. Jones have made helpful criticism of the manuscript.

REFERENCES

1. R. HILL, *Proc. Roy. Soc. London* **193A**, 281 (1948).
2. J. F. W. BISHOP and R. HILL, *Phil. Mag.* **42**, 414 and 1298 (1951).
3. G. I. TAYLOR, *J. Inst. Metals* **62**, 307 (1938).
4. G. Y. CHIN, W. L. MAMMEL and M. J. DOLAN, *Trans. TMS-AIME* **239**, 1111 and 1854 (1967).
5. G. Y. CHIN and W. L. MAMMEL, *Trans. AIME* **239**, 1400 (1967).
6. J. W. HUTCHINSON, *J. Mech. Phys. Solids TMS* **12**, 11 and 25 (1964).
7. P. PENNING, *Met. Trans.* **7A**, 1021 (1976).
8. P. PARNIERE and C. SAUZAY, *Mat. Sci. Engng* **22**, 271 (1976).
9. C. S. DA VIANA, J. S. KALLEND and G. J. DAVIES, *Int. J. Mech. Sci.* **21**, 355 (1979).
10. H. R. PIEHLER and W. A. BACKOFEN, In *Textures in Research and Practice* (Edited by J. Grewen and G. Wasserman), p. 436. Springer Verlag, Berlin (1961); Also H. R. PIEHLER, *Sc.D. Thesis, Mass. Inst. of Tech.* (1967).
11. H. R. PIEHLER and W. A. BACKOFEN, *Met. Trans.* **2**, 249 (1971).
12. J. M. ROSENBERG and H. R. PIEHLER, *Met. Trans.* **2**, 257 (1971).
13. S. L. SEMIATIN and P. R. MORRIS, *Texture Cryst. Sol.* **3**, 113 (1979).
14. S. L. SEMIATIN, P. R. MORRIS and H. R. PIEHLER, *Texture Cryst. Sol.* **3**, 191 (1979).
15. D. J. WILDE, *Optimum Searching Methods*, p. 32. Prentice-Hall, Englewood Cliffs, New Jersey (1964).
16. B. PAUL, In *Fracture, An Advanced Treatise, Mathematical Fundamentals* (Edited by Liebowitz), Vol. 2, p. 346. Academic Press, New York (1968).
17. W. F. HOSFORD, *J. Appl. Mech. Trans. ASME* **E39**, 607 (1972).
18. W. F. HOSFORD, *Proc. 7th North American Metal Working Research Conf*, p. 191. Society of Manufacturing Engineers, Dearborn, Michigan (1979).
19. R. HILL, *Math. Proc. Camb. Phil. Soc.* **75**, 179 (1979).
20. R. PEARCE, *Int. J. Mech. Sci.* **10**, 995 (1968).
21. J. WOODTHORPE and R. PEARCE, *Int. J. Mech. Sci.* **12**, 341 (1970).
22. A. PARMAR and P. B. MELLOR, *Int. J. Mech. Sci.* **20**, 385 (1978).
23. A. PARMAR and P. B. MELLOR, In *Mechanics of Sheet Metal Forming* (Edited by D. P. Koistinen and N. Wang), p. 53. Plenum Press, New York (1978).
24. J. L. BASSANI, *Int. J. Mech. Sci.* **19**, 651 (1977).